Title
SOURCE PROVENANCE OF OBSIDIAN CRUCIFORMS FROM THE SOUTHERN U.S. SOUTHWEST

Author
Shackley, M. Steven

Publication Date
2021-09-23

GEOARCHAEOLOGICAL XRF LAB
A GREEN SOLAR FACILITY

GEOARCHAEOLOGICAL X-RAY FLUORESCENCE SPECTROMETRY LABORATORY
8100 WYOMING BLVD., SUITE M4-158 ALBUQUERQUE, NM 87113 USA

SOURCE PROVENANCE OF OBSIDIAN CRUCIFORMS FROM THE SOUTHERN U.S. SOUTHWEST

by

M. Steven Shackley, Ph.D., Director
Geoarchaeological XRF Laboratory
Albuquerque, New Mexico

Report Prepared for

John Roney
Albuquerque, New Mexico

28 September 2021

INTRODUCTION

The analysis here of 21 obsidian cruciforms, and one cruciform produced from a volcanic or plutonic rock, from archaeological sites presumably from southern New Mexico and northern Chihuahua indicates a diverse provenance assemblage dominated by the northern Chihuahuan obsidian source at Sierra Fresnal (Shackley 2005). The remainder of the artifacts are produced from one of the sources in the Jemez Mountains of northern New Mexico, but likely procured from Rio Grande Quaternary alluvium (see Church 2000; Shackley 2021). A brief discussion is offered below.

ANALYSIS AND INSTRUMENTATION

All archaeological samples are analyzed whole. The results presented here are quantitative in that they are derived from "filtered" intensity values ratioed to the appropriate x-ray continuum regions through a least squares fitting formula rather than plotting the proportions of the net intensities in a ternary system (McCarthy and Schamber 1981; Schamber 1977). Or more essentially, these data through the analysis of international rock standards, allow for inter-instrument comparison with a predictable degree of certainty (Hampel 1984; Shackley 2011).

All analyses for this study were conducted on a ThermoScientific *Quant'X* EDXRF spectrometer, located at the Geoarchaeological XRF Laboratory, Albuquerque, New Mexico. It is equipped with a thermoelectrically Peltier cooled solid-state Si(Li) X-ray detector, with a 50 kV, 50 W, ultra-high-flux end window bremsstrahlung Rh target X-ray tube and a 76 µm (3 mil) beryllium (Be) window (air cooled), that runs on a power supply operating from 4-50 kV/0.02-1.0 mA at 0.02 increments. The spectrometer is equipped with a 200 l min^{-1} Edwards vacuum pump, allowing for the analysis of lower-atomic-weight elements between sodium (Na) and

titanium (Ti). Data acquisition is accomplished with a pulse processor and an analogue-to-digital converter. Elemental composition is identified with digital filter background removal, least squares empirical peak deconvolution, gross peak intensities and net peak intensities above background.

Trace Element Analysis

The analysis for mid Zb condition elements Ti-Nb, Pb, Th, the x-ray tube is operated at 30 kV, using a 0.05 mm (medium) Pd primary beam filter in an air path at 100 seconds livetime to generate x-ray intensity $K\alpha_1$-line data for elements titanium (Ti), manganese (Mn), iron (as $Fe_2O_3^T$), cobalt (Co), nickel (Ni), copper, (Cu), zinc, (Zn), gallium (Ga), rubidium (Rb), strontium (Sr), yttrium (Y), zirconium (Zr), niobium (Nb), lead (Pb), and thorium (Th). Not all these elements are reported since their values in many volcanic rocks are very low. Trace element intensities were converted to concentration estimates by employing a linear calibration line ratioed to the Compton scatter established for each element from the analysis of international rock standards certified by the National Institute of Standards and Technology (NIST), the US. Geological Survey (USGS), Canadian Centre for Mineral and Energy Technology, and the Centre de Recherches Pétrographiques et Géochimiques in France (Govindaraju 1994). Line fitting is linear (XML) for all elements. When barium (Ba) is analyzed in the High Zb condition, the Rh tube is operated at 50 kV and up to 1.0 mA, ratioed to the bremsstrahlung region (see Davis 2011; Shackley 2011a). Further details concerning the petrological choice of these elements in Southwest obsidians is available in Shackley (1988, 1995, 2005; also Mahood and Stimac 1991; and Hughes and Smith 1993). Nineteen specific pressed powder standards are used for the best fit regression calibration for elements Ti-Nb, Pb, Th, and Ba, and include G-2 (basalt), AGV-2 (andesite), GSP-2 (granodiorite), SY-2 (syenite), BHVO-2 (hawaiite), STM-1 (syenite), QLO-1 (quartz latite), RGM-1 (obsidian), W-2 (diabase),

BIR-1 (basalt), SDC-1 (mica schist), TLM-1 (tonalite), SCO-1 (shale), NOD-A-1 and NOD-P-1 (manganese) all US Geological Survey standards, NIST-278 (obsidian), U.S. National Institute of Standards and Technology, BE-N (basalt) from the Centre de Recherches Pétrographiques et Géochimiques in France, and JR-1 and JR-2 (obsidian) from the Geological Survey of Japan (Govindaraju 1994).

Major and Minor Oxide Analysis

Analysis of the major oxides of Si, Al, Ca, Fe, K, Mg, Mn, Na, and Ti is performed under the multiple conditions elucidated below. This fundamental parameter analysis (theoretical with standards), while not as accurate as destructive analyses (pressed powder and fusion disks) is usually within a few percent of actual, based on the analysis of USGS RGM-1 obsidian or in this study the USGS AGV-1 andesite standard (see also Shackley 2011b). The fundamental parameters (theoretical) method is run under conditions commensurate with the elements of interest and calibrated with 11 USGS standards (RGM-1, rhyolite; AGV-2, andesite; BHVO-1, hawaiite; BIR-1, basalt; G-2, granite; GSP-2, granodiorite; BCR-2, basalt; W-2, diabase; QLO-1, quartz latite; STM-1, syenite), and one Japanese Geological Survey rhyolite standard (JR-1). See Lundblad et al. (2011) for another set of conditions and methods for oxide analyses.

Conditions Of Fundamental Parameter Analysis[1]:

Low Za (Na, Mg, Al, Si, P)

Voltage	6 kV	Current	Auto[2]
Livetime	100 seconds	Counts Limit	0
Filter	No Filter	Atmosphere	Vacuum
Maximum Energy	10 keV	Count Rate	Low

Mid Zb (K, Ca, Ti, V, Cr, Mn, Fe)

Voltage	32 kV	Current	Auto
Livetime	100 seconds	Counts Limit	0
Filter	Pd (0.06 mm)	Atmosphere	Vacuum
Maximum Energy	40 keV	Count Rate	Medium

High Zb (Sn, Sb, Ba, Ag, Cd)

Voltage	50 kV	Current	Auto
Livetime	100 seconds	Counts Limit	0
Filter	Cu (0.559 mm)	Atmosphere	Vacuum
Maximum Energy	40 keV	Count Rate	High

Low Zb (S, Cl, K, Ca)

Voltage	8 kV	Current	Auto
Livetime	100 seconds	Counts Limit	0
Filter	Cellulose (0.06 mm)	Atmosphere	Vacuum
Maximum Energy	10 keV	Count Rate	Low

[1] Multiple conditions designed to ameliorate peak overlap identified with digital filter background removal, least squares empirical peak deconvolution, gross peak intensities and net peak intensities above background.
[2] Current is set automatically based on the mass absorption coefficient.

The data from the WinTrace software were translated directly into Excel for Windows and into SPSS ver. 27 and JMP 12.0.1 for statistical manipulation. The USGS rhyolite standard RGM-1 is analyzed during each sample run of ≤ 19 samples for obsidian artifacts to evaluate machine calibration (Table 1). Source assignments were made by reference to source data at http://swxrflab.net/swobsrcs.htm, (see also Shackley 1995, 2005, 2021; Shackley et al. 2018).

DISCUSSION

Artifacts produced from sources present in the collection while seemingly from a large area of the North American Southwest, are likely all from the southern portion of New Mexico or the northern portion of Chihuahua. All the sources from the Jemez Mountains and Mount Taylor volcanic fields in northern New Mexico are present in the Quaternary alluvium of the Rio Grande as far south as Chihuahua (Church 2000; Shackley 2021). While the primary source for Sierra Fresnal obsidian is the mountain range by the same name in north-central Chihuahua, it is also available as secondary deposits in the Rio Nuevo Casas Grandes nearer the border (Shackley 2005). It is always difficult to determine whether the raw material for a given artifact was procured from the primary source through exchange or directly, the first approximation is that the nearest available source is the most likely, as shown recently in archaeological contexts between Pojoaque, and Las Cruces New Mexico (Shackley 2021).

Sierra Fresnal

Nearly 50% (47.6%) of the assemblage was produced from the Sierra Fresnal source, a large set of coalesced rhyolite domes near Lago Fresnal and Lago Guzman (see Shackley 2005:83-84; Tables 1 and 2 here). This is one of the few known sources in Chihuahua with a known primary location, and its elemental composition is calc-alkalic and not peralkaline, and appears to not be part of the Sierra Madre volcanic province (Murray et al. 2014; Ferrari et al. 2007; Figure 1 here). The nodules have eroded north at least as far as Nuevo Casas Grandes and into Lago Fredrico to the west of Sierra Fresnal. Five of the nodules collected by Alan Phelps at Lago Fredrico are now considered part of the Sierra Fresnal source. It does occur in various archaeological contexts north of the border, and appears to be one of the major sources in the region (Dolan et al. 2017a, 2017b, 2019; Shackley 2005).

Jemez Lineament Sources

The four sources from the two Jemez Lineament volcanic fields (Jemez and Mount Taylor) including Cerro Toledo Rhyolite (23.8%), El Rechuelos Rhyolite (9.5%), Canovas Canyon Rhyolite (4.8%), and Grants Ridge at Mount Taylor (4.8%) are commonly recovered in Rio Grande Quaternary alluvium (Church 2000; Shackley 2021; Tables 1 and 2 and Figure 1 here). The Mount Taylor sources only enter the Rio Grande from the Rio Puerco near Socorro, New Mexico. Cerro Toledo Rhyolite obsidian is the most common in Rio Grande gravels due to the violent nature of the Cerro Toledo eruptive event and entering the Rio Grande at multiple points along the river basin (Shackley 2021).

Other Unlocated Source

Nearly 10% of the artifacts were produced from an as yet unlocated source likely somewhere in Chihuahua (Tables 1 and 2; see Fralick et al. 1998; Figure 1 here). This source has not appeared in archaeological contexts to my knowledge including those north of the border. It does not match any of the 160,000+ sources in the Skinner/Shackley database of North American obsidian sources.

The Silicic Plutonic or Volcanic Rock Sample

Sample DA9 appears to be a high silica volcanic or plutonic rock (Figure 2). Given the highly polished character it is difficult to determine the exact rock type, but the size of the mineral components argue for a plutonic rock likely granite (see Figure 2). The composition is similar to most grantitoid rocks common in the North American Southwest. It is definitely not a high calcium sediment.

REFERENCES CITED

Church, T.
2000 Distribution and Sources of Obsidian in the Rio Grande Gravels of New Mexico. *Geoarchaeology* 15:649-678.

Davis, M.K., T.L. Jackson, M.S. Shackley, T. Teague, and J. Hampel
2011 Factors Affecting the Energy-Dispersive X-Ray Fluorescence (EDXRF) Analysis of Archaeological Obsidian. In *X-Ray Fluorescence Spectrometry (XRF) in Geoarchaeology*, edited by M.S. Shackley, pp. 45-64. Springer, New York.

Dolan, S.G., M.E. Whalen, P.E. Minnis, and M.S. Shackley
2017a Obsidian in the Casas Grande World: Procurement, Exchange, and Interaction in Chihuahua, Mexico, CE 1200-1450. *Journal of Archaeological Science Reports* 11:555- 567.

Dolan, S.G., M.R. Miller, M.S. Shackley, and K. Corl
2017b El Paso Phase Obsidian Procurement in southern New Mexico: Implications for Jornada Mogollon Regional Interaction and Exchange. *Kiva* 83:267-291.

Dolan, S.G., E. Gallaga, and M.S. Shackley
2019 Obsidian Provenance Data Reveals New Insights into Archaic Lifeways in Chihuahua, Mexico. *Lithic Technology* 44:237-256.

Ferrari, Luca, Martín Valencia-Moreno, and Scott Bryan
2007 Magmatism and Tectonics of the Sierra Madre Occidental and Its Relation with the Evolution of the Western Margin of North America. In *Geology of Mexico: Celebrating the Centenary of the Geological Society of Mexico*, edited by Susana A. Alaniz-Álvarez and Ángel F. Nieto-Samaniego, pp. 1–39. The Geological Society of America Special Paper 422. Boulder, Colorado.

Fralick, P.W., J.D. Stewart, and A.C. MacWilliams
1998 Geochemistry of the West-Central Chihuahua Obsidian Nodules and Implications for the Derivation of Obsidian Artefacts. *Journal of Archaeological Science* 25:1023-1038.

Govindaraju, K.
1994 1994 Compilation of Working Values and Sample Description for 383 Geostandards. *Geostandards Newsletter* 18 (special issue).

Hampel, Joachim H.
1984 Technical Considerations in X-ray Fluorescence Analysis of Obsidian. In *Obsidian Studies in the Great Basin*, edited by R.E. Hughes, pp. 21-25. Contributions of the University of California Archaeological Research Facility 45. Berkeley.

Hildreth, W.
1981 Gradients in Silicic Magma Chambers: Implications for Lithospheric Magmatism. *Journal of Geophysical Research* 86:10153-10192.

Hughes, Richard E., and Robert L. Smith
1993 Archaeology, Geology, and Geochemistry in Obsidian Provenance Studies. *In Scale on Archaeological and Geoscientific Perspectives*, edited by J.K. Stein and A.R. Linse, pp. 79-91. Geological Society of America Special Paper 283.

Mahood, Gail A., and James A. Stimac
1990 Trace-Element Partitioning in Pantellerites and Trachytes. *Geochemica et Cosmochimica Acta* 54:2257-2276.

McCarthy, J.J., and F.H. Schamber
1981 Least-Squares Fit with Digital Filter: A Status Report. In *Energy Dispersive X-ray Spectrometry*, edited by K.F.J. Heinrich, D.E. Newbury, R.L. Myklebust, and C.E. Fiori, pp. 273-296. National Bureau of Standards Special Publication 604, Washington, D.C.

Murray, B.P., C.J. Busby, M. de los Angeles Verde Ramirez
2014 Extension and Magmatism in the Cerocahui Basin, northern Sierra Madre Occidental, western Chihuahua, Mexico. *International Geology Review* 57:893-918.

Schamber, F.H.
1977 A Modification of the Linear Least-Squares Fitting Method which Provides Continuum Suppression. In *X-ray Fluorescence Analysis of Environmental Samples*, edited by T.G. Dzubay, pp. 241-257. Ann Arbor Science Publishers.

Shackley, M. Steven
1988 Sources of Archaeological Obsidian in the Southwest: An Archaeological, Petrological, and Geochemical Study. *American Antiquity* 53:752-772.

1995 Sources of Archaeological Obsidian in the Greater American Southwest: An Update and Quantitative Analysis. *American Antiquity* 60:531-551.

2005 *Obsidian: Geology and Archaeology in the North American Southwest*. University of Arizona Press, Tucson.

2011 An Introduction to X-Ray Fluorescence (XRF) Analysis in Archaeology. In *X-Ray Fluorescence Spectrometry (XRF) in Geoarchaeology*, edited by M.S. Shackley, pp. 7-44. Springer, New York.

2021 Distribution and Sources of Secondary Deposit Archaeological Obsidian in Rio Grande Alluvium New Mexico, USA. *Geoarchaeology* 36:808-825.

Shackley, M.S., L.E. Morgan, and D. Pyle
2018 Elemental, Isotopic, and Geochronological Variability in Mogollon-Datil Volcanic Province Archaeological Obsidian, Southwestern USA: Solving Issues of Inter-Source Discrimination. *Geoarchaeology* 33:486-497.

Table 1. Elemental concentrations and source assignments for the obsidian artifacts and USGS RGM-1 rhyolite standard. All measurements in weight percent (%) or parts per million (ppm) as noted.

Sample	Ti ppm	Mn ppm	Fe ppm	Rb ppm	Sr ppm	Y ppm	Zr ppm	Nb ppm	Ba ppm	Ce ppm	Pb ppm	Th ppm	Source
DA1	1307	350	11290	303	44	62	166	43	217	108	26	47	Sierra Fresnal, CHIH
DA2	1645	553	13504	298	44	64	166	37	222	128	29	36	Sierra Fresnal, CHIH
DA3	1254	348	11649	304	37	63	160	36	220	91	23	50	Sierra Fresnal, CHIH
DA5	1018	396	8149	153	12	23	72	49	17	35	23	20	El Rechuelos Rhy, NM
DA6	1211	344	11490	313	49	69	182	39	251	173	24	44	Sierra Fresnal, CHIH
DA7	1153	425	9074	122	44	24	116	51	442	67	28	21	Canovas Canyon Rhy, NM
DA10	982	469	7748	185	14	29	74	58	18	48	29	12	El Rechuelos Rhy, NM
DA11	1347	323	11706	319	49	64	172	33	237	155	25	45	Sierra Fresnal, CHIH
DA13	909	482	10455	196	12	58	171	95	7	76	32	16	Cerro Toledo Rhy, NM
DA14	1164	308	10710	295	40	63	163	37	182	91	24	43	Sierra Fresnal, CHIH
DA15	926	697	9346	525	13	75	118	184	34	29	55	22	Grants Ridge, Mt Taylor, NM
DA16	1483	396	10547	231	28	47	246	23	528	101	26	32	unknown
DA17	952	491	11019	214	9	63	180	100	2	59	30	26	Cerro Toledo Rhy, NM
DA18	1275	347	11244	287	42	58	156	30	197	133	29	38	unknown
DA19	1529	412	10449	233	29	45	239	27	524	104	25	17	unknown
DA20	1234	349	11508	303	47	60	164	39	211	122	25	46	Sierra Fresnal, CHIH
DA22	1305	306	11398	295	42	61	168	41	210	104	21	49	Sierra Fresnal, CHIH
DA24	1314	355	11972	304	46	62	172	40	202	96	25	47	Sierra Fresnal, CHIH
DA25	982	450	10418	198	9	62	163	99	3	41	33	17	Cerro Toledo Rhy, NM
MARSHALL A	935	463	10947	202	11	59	172	99	0	40	30	18	Cerro Toledo Rhy, NM
MARSHALL B	1148	482	11195	193	14	60	173	89	0	51	32	22	Cerro Toledo Rhy, NM
RGM1-S4	1618	295	13373	151	110	23	228	8	780	27	22	17	standard

	Na2O %	MgO %	Al2O3 %	SiO2 %	P2O5 %	K2O %	CaO %	TiO2 %	V2O5 %	Cr2O3 %	MnO %	Fe2O3 %	∑
DA9	3.78	0.19	10.42	74.24	0.00	5.64	0.70	0.18	0.02	0.00	0.12	4.29	99.57
RGM1-S4	4.05	0.00	13.11	73.79	0.00	4.87	1.42	0.27	0.02	0.01	0.04	2.22	99.79

Table 2. Frequency distribution of obsidian sources in the assemblage.

Source	Frequency	Percent
Sierra Fresnal, CHIH	10	47.6
Cerro Toledo Rhy, NM	5	23.8
El Rechuelos Rhy, NM	2	9.5
Canovas Canyon Rhy, NM	1	4.8
Grants Ridge, Mt Taylor, NM	1	4.8
unknown	2	9.5
Total	**21**	**100.0**

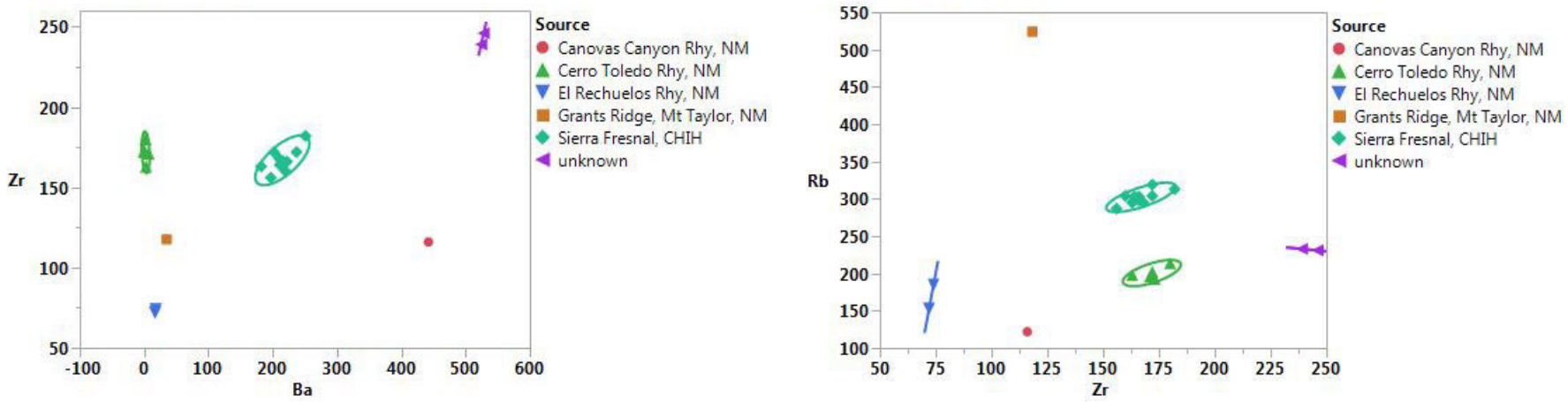

Figure 1. Ba/Zr and Zr/Rb bivariate plots of the archaeological samples. Confidence ellipses at 90%.

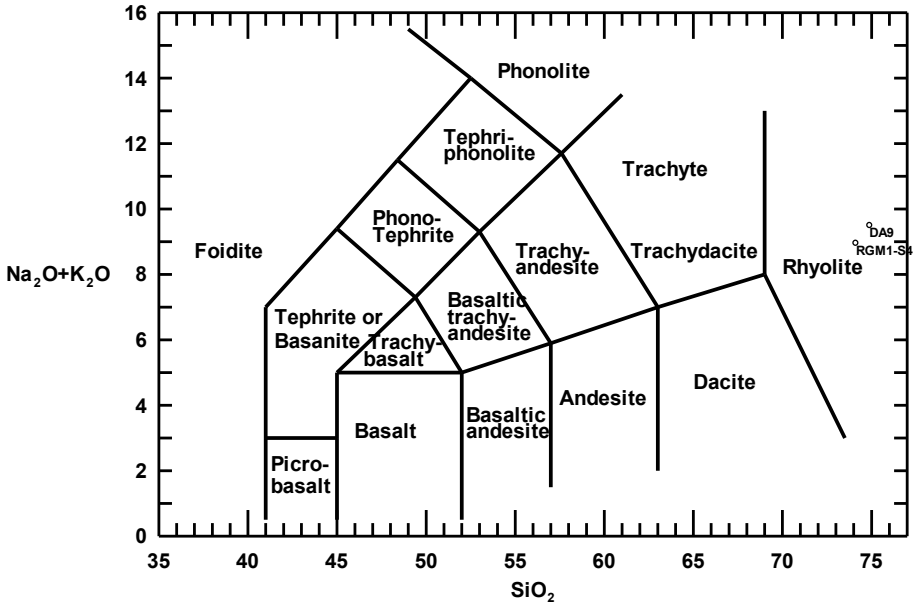

Figure 2. TAS plot of sample DA9 and USGS RGM-1 rhyolite standard.